



**UNIVERSIDADE ESTADUAL DE CAMPINAS
SISTEMA DE BIBLIOTECAS DA UNICAMP
REPOSITÓRIO DA PRODUÇÃO CIENTÍFICA E INTELLECTUAL DA UNICAMP**

Versão do arquivo anexado / Version of attached file:

Versão do Editor / Published Version

Mais informações no site da editora / Further information on publisher's website:

<https://aip.scitation.org/doi/10.1063/1.5052226>

DOI: 10.1063/1.5052226

Direitos autorais / Publisher's copyright statement:

©2019 by AIP Publishing. All rights reserved.

DIRETORIA DE TRATAMENTO DA INFORMAÇÃO

Cidade Universitária Zeferino Vaz Barão Geraldo

CEP 13083-970 – Campinas SP

Fone: (19) 3521-6493

<http://www.repositorio.unicamp.br>

Complex magnetic behavior along the GdIn (Ni_xCu_{1-x})₄ (0.00 ≤ x ≤ 1.00) series of compounds

Cite as: J. Appl. Phys. 125, 063903 (2019); doi: 10.1063/1.5052226

Submitted: 15 August 2018 · Accepted: 22 January 2019 ·

Published Online: 13 February 2019



S. G. Mercena,¹  E. C. Mendonça,¹ C. T. Meneses,¹  L. S. Silva,^{1,2} J. G. S. Duque,^{1,3} C. B. R. Jesus,^{1,3} J. C. Souza,³ and P. G. Pagliuso³

AFFILIATIONS

¹Programa de Pós-Graduação em Física, Campus Prof. José Aluísio de Campos, UFS, 49100-000 São Cristóvão, SE, Brazil

²Instituto Federal de Tocantins, IFTO, Campus Colinas do Tocantins, 77760-000 Colinas do Tocantins, TO, Brazil

³Instituto de Física “Gleb Wataghin,” UNICAMP, 13083-970, Campinas-São Paulo, Brazil

ABSTRACT

In this work, structural, magnetic, and local properties of GdIn(Ni_xCu_{1-x})₄ (0.00 ≤ x ≤ 1.00) samples synthesized via the flux method are investigated by means of X-ray, magnetization, specific heat, and electron spin resonance measurements. The analysis of X-ray powder diffraction data taken at room temperature reveals that all samples belong to the cubic space group (Cl5b-type structure) with lattice parameters, *a*, ranging from 7.08 < *a* < 7.23 Å. Interestingly, the analysis of both *T*-dependence magnetic susceptibility and *MvsH* loops indicates a gradual transition from antiferromagnetic to ferromagnetic ground states as a function of the Ni-doping. The transition temperatures are confirmed via specific heat measurements. Finally, electron spin resonance data taken in the temperature range of 100 ≤ *T* ≤ 300 K show a single Dysonian line shape, which is characteristic of a metallic environment. A nearly *T*-independent *g*-value was observed and the value was concentration independent. Besides, the doped samples show an increase of the residual linewidth, which can be linked with the chemical disorder introduced by the Ni-doping. Our results are discussed considering the bottleneck and multiple band effects on the Gd³⁺ spin dynamics in this series and their implication in the magnetic frustration observed in these materials.

Published under license by AIP Publishing. <https://doi.org/10.1063/1.5052226>

I. INTRODUCTION

It is well established that the magnetic behavior of localized 4*f* electrons in metallic systems can be fairly explained by the framework of the Ruderman-Kittel-Kasuya-Yoshida (RKKY) theory where the magnetic moment of 4*f* electrons is coupled via the conduction electrons (*ce*).¹⁻³ However, this theory does not fully describe the properties of systems with partly localized *f*-electrons, such as Ce and Yb-based intermetallic compounds. Besides being responsible for the magnetically ordered states, the 4*f* electrons can participate in other interesting physical phenomena such as Kondo effect heavy-fermion states, unconventional superconductivity, non-Fermi liquid behavior, and intermediate valency.⁴⁻¹⁰ In fact, despite its success in predicting the magnetic order of a broad variety of materials, the RKKY approach has failed to correctly describe the magnetic ground state for many materials found in the literature,¹¹⁻¹³ even for systems claimed to have completely localized 4*f* electrons. For instance, the simple application of the RKKY model fails in predicting the magnetic ground state

for the family of compounds Yb(Au,In,Pd)A₄ (A = Cu, Ni).¹⁴ In particular, magnetization, specific heat, and resistivity measurements indicate that the ferromagnetic order develops in a doublet crystal-field (CF) ground state for the YbInNi₄ compound, while a simple analysis based on the RKKY model yields an antiferromagnetic order for YbInNi₄.¹⁵ This fact may be an indication that a more careful analysis of the Friedel-type model¹⁶ must be used for these materials. The inclusion of magnetic interaction terms larger than nearest-neighbor and a more realistic treatment of the electronic band structure must be added in order to better describe the correct magnetic ground states. For instance, the contribution of *ce* coming from different bands *s*, *p*, *d*, or even *f* should be properly taken into account in the RKKY theory. In this respect, it is important to comment that experimental results of the electron paramagnetic resonance of Gd³⁺ ions diluted in LuInA₄ (A = Cu, Ni) show a sign change of the exchange parameter, *J*_{*f-ce*}, between the *ce* and the 4*f* localized moments. This has been discussed based on a single *s*-band model for A = Cu and a two band

model, s and d , for $A = \text{Ni}$.¹⁷ This finding can be indicative that multiple bands theory must be taken into account to explain the microscopic magnetic interaction and so the ground states of these concentrated $4f$ electrons systems.

In this sense, the cubic AuBe_5 ($C15b$, $F43m$)-type structure^{18,19} GdInA_4 ($A = \text{Cu, Ni}$) compounds are particularly interesting due to their well-localized Gd spins with no orbital moment forming an fcc lattice. Therefore, the absence of crystal field (CF) effects can be important to test the issues mentioned above. It is well known that GdInCu_4 presents an antiferromagnetic order at $T = 5.5 \text{ K}$ ²⁰ and, due to its particular crystal symmetry, the frustration phenomena give rise.^{18,19,21} This means that not all magnetic interactions between next-neighbor can be minimized simultaneously and, consequently, the observed order temperature, T_N , is much lower than the Curie-Weiss temperature, Θ_{CW} . On the other hand, the $\text{Gd}(\text{Au,In,Pd})\text{Ni}_4$ variants are relatively unexplored.

In order to further investigate the evolution of the magnetic properties along this series of compounds, we have synthesized the $\text{GdIn}(\text{Ni}_x\text{Cu}_{1-x})_4$ ($0.00 \leq x \leq 1.00$) series of compounds. Samples have been characterized via X-ray diffraction, magnetization, specific heat, and electron spin resonance (ESR) measurements. The X-ray analysis shows that all samples have a cubic crystal symmetry ($C15b$ - AuBe_5) with a lattice parameter, a , in the range $7.08 \leq a \leq 7.23 \text{ \AA}$. The magnetic susceptibility as a function of temperature and applied magnetic field point out to an antiferromagnetic order for Cu-rich samples, while the Ni-rich samples display a ferromagnetic order with magnetization saturation close to the expected theoretically value of $7.94 \mu_B$. Finally, the ESR spectra consist of a single Dysonian lineshape, which is characteristic of localized moments in a metallic host. In comparison with GdInCu_4 , the residual linewidth increases with Ni-doping. This increase can be linked with the disorder degree induced by the doping. Furthermore, the evolution of the Gd^{3+} ESR Korringa-like rate b along the series suggests the presence of multiple band effects, which may play an important role in driving the system to a ferromagnetic ground state, resulting in a breakdown of the magnetic frustration.

II. EXPERIMENT

Single crystals of $\text{GdIn}(\text{Ni}_x\text{Cu}_{1-x})_4$ ($0.00 \leq x \leq 1.00$) were grown from a Cu/Ni-In-flux method. Starting elements with purities of 99.9% in a molar ratio of 1(Gd):2(In):5(Ni, Cu) were placed into an alumina crucible and sealed under vacuum in a quartz tube. The ampules were then heated in the temperature range $1100 < T < 1175 \text{ }^\circ\text{C}$, kept at this temperature for 5 h, and slowly cooled down at $5 \text{ }^\circ\text{C/h}$ up to $650 \text{ }^\circ\text{C}$ (for Cu-rich samples) and $950 \text{ }^\circ\text{C}$ (for Ni-rich samples) where the excess of flux was decanted off from the cubic-like crystals by centrifugation. X-ray powder diffraction measurements carried out at room temperature were used to check the sample quality and phase purity. The magnetic susceptibility data were taken using a commercial dc superconducting quantum interference device (SQUID) magnetometer. It is important to say that all magnetization measurements were carried out in

powder samples. Specific heat measurements were performed in a commercial small-mass calorimeter system that employs a quasiadiabatic thermal relaxation technique for samples ranged from 5 to 30 mg. The ESR experiments were done in powder samples using a commercial X-band spectrometer ($f = 9.48 \text{ GHz}$) with the TE_{102} cavity coupled to a He flow cryostat.

III. EXPERIMENTAL RESULTS AND DISCUSSION

Figure 1 shows the X-ray powder diffraction measurements carried out at room temperature for the $\text{GdIn}(\text{Ni}_x\text{Cu}_{1-x})_4$ ($0.00 \leq x \leq 1.00$) samples. The solid lines indicate the refined X-ray pattern using the Rietveld protocol (red) and the difference between experimental and theoretical data (blue). In the top inset, we show the photograph of a single crystal on a

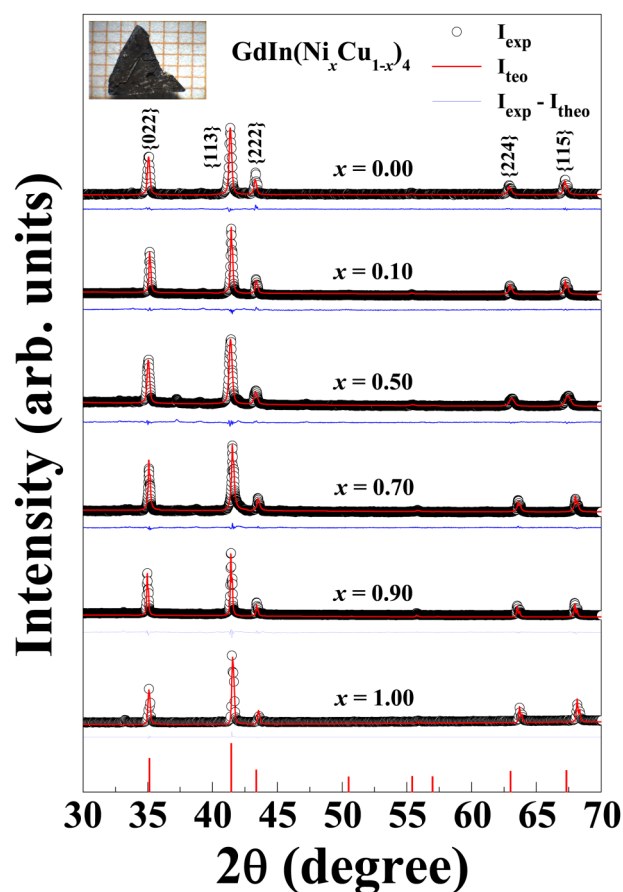


FIG. 1. X-ray powder diffraction measurements carried out at room temperature for the $\text{GdIn}(\text{Ni}_x\text{Cu}_{1-x})_4$ ($0.00 \leq x \leq 1.00$) samples. The red solid lines are the fits obtained by using the Rietveld method and the blue ones represent the difference between experimental and calculated patterns. The vertical bars mean the standard pattern found in the Inorganic Crystal Structure Database (ICSD 627.611). In the top inset, we show the photograph of a single crystal on a mm grid.

TABLE I. The goodness-of-fit parameters (R_w , R_{wp} , and χ^2); lattice parameter, a ; volume, V ; Néel and Curie-Weiss temperatures, T_N ; Θ_{CW} ; p ; f parameter; b [$= \Delta H/\Delta T$ (Oe/K)], and g -value extracted from best fits to our set of X-ray, susceptibility, and ESR data.

x	R_p (%)	R_{wp} (%)	χ^2 (%)	a (Å)	V (g/cm ³)	T_N (K)	Θ_{CW} (K)	p	f	b (Oe/K)	g -value
0.00	6.33	8.30	3.30	7.2331(2)	378.42(3)	6	-51	7.83	8.5	0.4(1)	1.995(5)
0.10	3.68	4.66	2.29	7.2356(2)	378.82(2)	4	-32	7.96	8.6	4(1)	1.99(1)
0.50	4.01	5.20	2.62	7.1866(5)	371.18(4)	8	-3	7.96	0.3	5(1)	2.01(2)
0.70	7.20	9.48	3.89	7.0921(3)	356.71(2)	6	-2	7.96	0.3	4(1)	1.99(1)
0.90	3.09	3.82	1.86	7.079(1)	354.70(1)	5	3	7.84	0.5	4(1)	2.01(2)
1.00	2.34	5.77	3.71	7.0873(5)	355.99(5)	5	3	7.78	0.6	4(1)	2.00(1)

mm grid. The analyses of X-ray patterns confirm that all samples crystallize in the cubic $AuBe_5$ structure ($C15b$ -type structure). The lattice parameters, a , were found in the range from $7.08 < a < 7.23$ Å (see Table I). One must note that there is a slight change in a as a function of Ni-doping. The data coming from Rietveld refinement have been used to construct the unit cells through the VESTA software. This allows us to evaluate the Gd-Gd distances, d_{Gd-Gd} , nearest-neighbor, which vary ranging from 5.007 to 5.117 Å.

Figure 2(a) displays the T-dependence of the magnetic susceptibility $\chi(T)$ at $H = 1$ kOe for the $GdIn(Ni_xCu_{1-x})_4$ ($0.00 \leq x \leq 1.00$) samples. The inset shows, in detail, the low

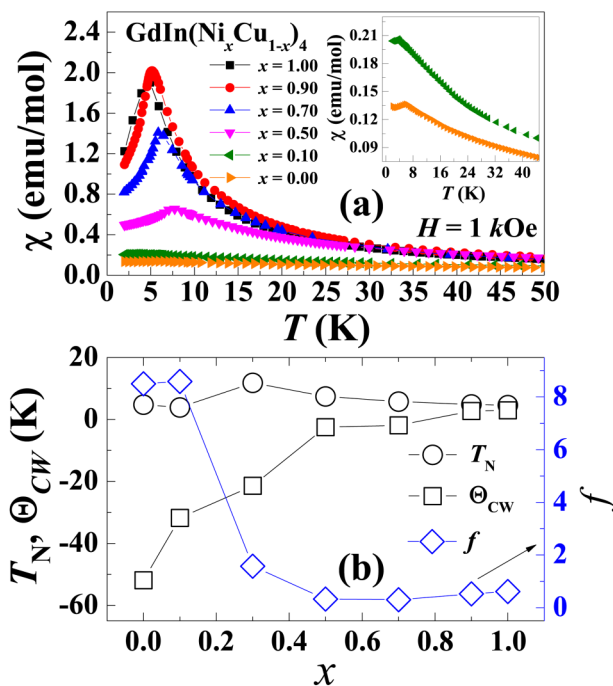


FIG. 2. (a) dc magnetic susceptibility, χ_{dc} , versus temperature from 2 to 50 K measured at $H = 1$ kOe for $GdIn(Ni_xCu_{1-x})_4$ ($0.00 \leq x \leq 1.00$) samples. In the inset, the $\chi(T)$ for Cu-rich samples are shown in the 2 to 45 K temperature range and (b) T_N , Θ_{CW} , and f as a function of Ni-doping concentration for $GdIn(Ni_xCu_{1-x})_4$.

temperature range for Cu-rich samples. Figure 2(b) shows the T_N , Θ_{CW} , and the parameter $f (= |\Theta_{CW}|/T_N)$ as a function of the Ni-doping. The magnetic susceptibility obeys the Curie-Weiss law over the temperature range from 100 K to room temperature for all samples. It is interesting to notice the strong variation of f along the family of materials [see Table I and Fig. 2(b)]. It is evident from these values that the magnetic frustration significantly decreases as a function of Ni-substitution, because f is almost 1 for highly concentrated Ni-doped samples. Moreover, one must observe that the Curie-Weiss temperatures are negative for Cu-rich samples, which indicates antiferromagnetic correlations. On the other hand, the positive values of Θ_{CW} obtained from fits of $\chi(T)$ for Ni-rich samples suggest that these compounds have a ferromagnetic ground state. It is worth to comment that, for the $YbInNi_4$ compound, inelastic neutron scattering²² and macroscopic measurements¹⁵ are consistent with a ferromagnetic order. However, it is well known that for $L \neq 0$ rare earth based compounds, the magnetic properties seem to be governed by both magnetic interactions and CF effects. At the $YbInNi_4$ compound, the magnetic order gives rise to a quartet/doublet crystal-field ground state.^{15,22}

Figure 3 shows the magnetization versus magnetic field for the $GdIn(Ni_xCu_{1-x})_4$ ($0 \leq x \leq 1.0$) samples measured at $T = 2$ K. It must be noted that for Ni-rich samples, the magnetization reaches a value of $6.9 \mu_B$, which is close to the Gd^{3+} theoretical magnetic moment of $7.94 \mu_B$. A linear behavior is observed up to $H = 70$ kOe for Cu-rich samples. The saturation in the H -dependent magnetization at 2 K is observed in the same concentration range where, according to the temperature dependent magnetic susceptibility curves, the Curie-Weiss temperatures are positive.

Figure 4 shows the magnetic contribution to the total specific heat (C_p) in the temperature range $0 < T < 30$ K for the $GdIn(Ni_xCu_{1-x})_4$ ($0 \leq x \leq 1.0$) samples at zero applied field. In the inset, we show the magnetic entropy, which was calculated integrating the magnetic specific heat. We used the $LuInCu_4$ compound as a non-magnetic reference to extract the phonon contribution of the total specific heat. The anomalies in the specific-heat data are associated with the onset of AFM/FM order, which are in good accordance with the transition temperatures extracted from the magnetic susceptibility data (see Table I).

Figure 5 shows the evolution of the X-band ($f \approx 9.45$ GHz) powder spectra of Gd^{3+} in $GdIn(Ni_xCu_{1-x})_4$ ($0 \leq x \leq 1.0$)

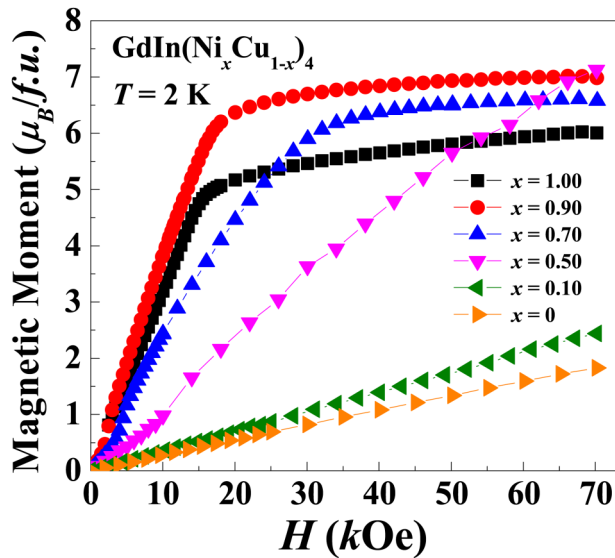


FIG. 3. Magnetization versus applied magnetic field for the $\text{GdIn}(\text{Ni}_x\text{Cu}_{1-x})_4$ ($0 \leq x \leq 1.0$) samples measured at $T = 2$ K.

measured at $T = 100$ K. We fitted the ESR spectra with an admixture of absorption and dispersive derivatives. The obtained result was a single Dysonian line shape (solid red lines). These line shapes are characteristic of localized magnetic moments in a metallic host with a skin depth smaller than the size of the sample.

Figure 6 shows the temperature dependence of the Gd^{3+} ESR linewidth, ΔH , as a function of temperature for the $\text{GdIn}(\text{Ni}_x\text{Cu}_{1-x})_4$ ($0.00 \leq x \leq 1.00$) samples. The thermal

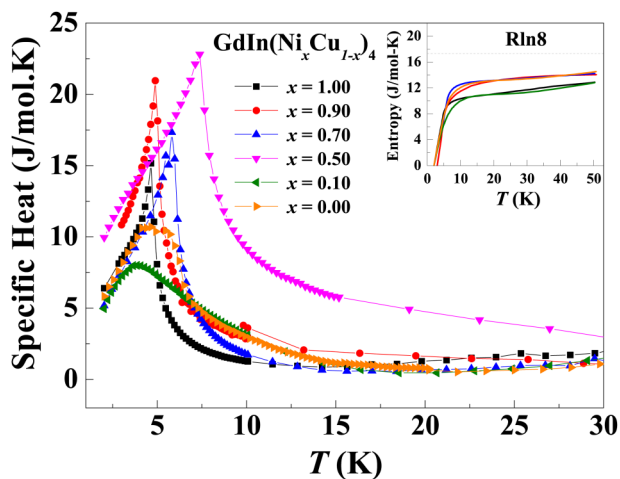


FIG. 4. Magnetic contribution to total specific heat for the $\text{GdIn}(\text{Ni}_x\text{Cu}_{1-x})_4$ ($0 \leq x \leq 1.0$) samples at zero applied field. In the inset, we show the magnetic entropy as a function of temperature.

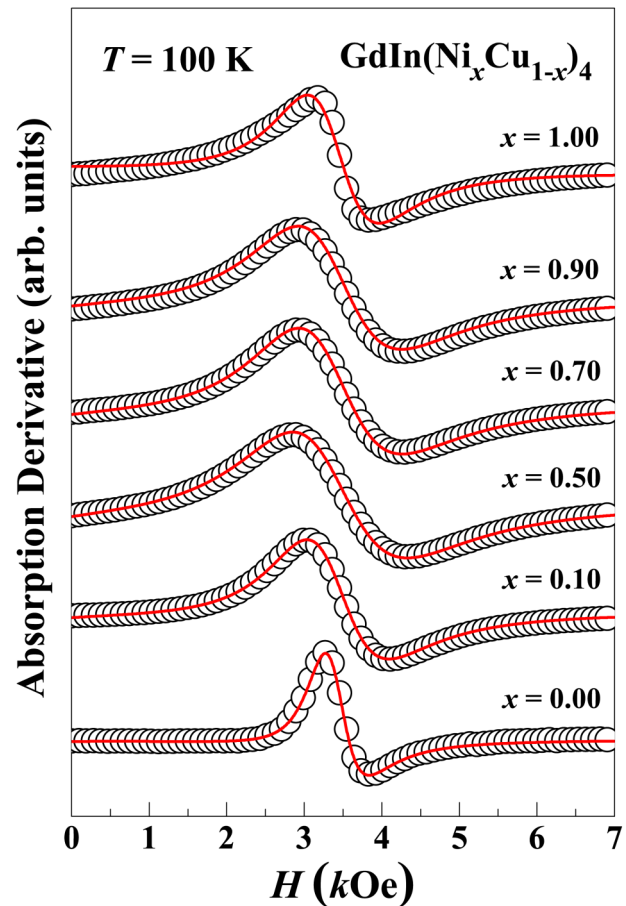


FIG. 5. Concentration evolution ($0 \leq x \leq 1.00$) of the ESR spectra in $\text{GdIn}(\text{Ni}_x\text{Cu}_{1-x})_4$ ($0 \leq x \leq 1.0$) measured at $T = 100$ K. The solid lines are the best fit of the resonance using a Dysonian lineshape.

broadening of the linewidths was fitted using $\Delta H = \Delta H_0 + bT$, where ΔH_0 is the residual linewidth and b is the Korringa-like rate. In the inset, we show the Ni dependence of ΔH_0 , which increases for intermediate members of the series indicating the introduction of significant disorder due to Ni-doping. The analysis of our ESR data, focused in the temperature range $100 < T < 300$ K, points out that there is almost no magnetic coupling of the Gd^{3+} spins due to a T -independent g -value (see Table 1) and a Korringa-like thermal broadening. Unfortunately, because of the relatively large Gd^{3+} ESR linewidth (and associated error in the experimental g -value) observed for both compounds, we were not able to determine the g -shift, which is related to the g -value of Gd^{3+} in insulators ($g = 1.993^{23}$). However, despite the Korringa-like rates remaining the same along the GdInA_4 ($A = \text{Cu}, \text{Ni}$) series, one can note a residual linewidth decreasing with the Ni-doping. As we have commented above, such effect can be linked with the disorder introduced by the doping.

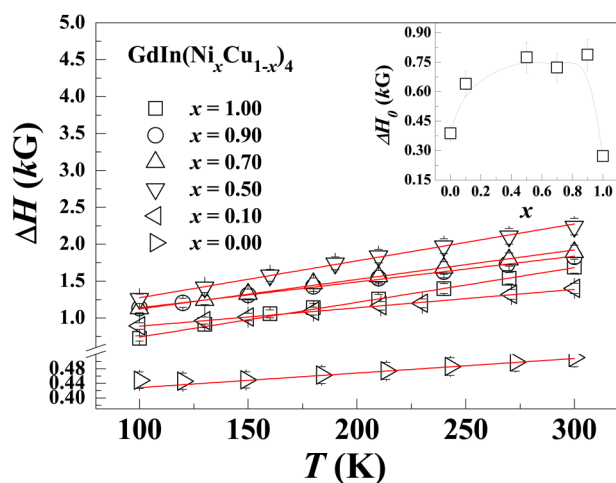


FIG. 6. Temperature dependence of the ESR linewidth for the $\text{GdIn}(\text{Ni}_x\text{Cu}_{1-x})_4$ ($0 \leq x \leq 1.0$) samples. The solid lines mean the best fit to the $\Delta H = \Delta H_0 + bT$. In the inset, we show the dependence on the residual linewidth as a function of the Ni concentration.

The evolution of b -rate, along the series, gives important insights regarding the complex magnetic properties of these systems. Firstly, the b -rate of the Gd^{3+} ESR linewidth in GdInCu_4 ($b \sim 0.4$ Oe/K) is somewhat smaller than the value of b found for diluted Gd^{3+} in LuInCu_4 ($b \sim 0.9$ Oe/K),¹⁷ indicating the presence of a moderate bottleneck effect.^{24,25} The b -rates increase by an order of magnitude, reaching a value of $b \sim 4$ Oe/K, when Ni is introduced into the Cu site. This Korringa-like rate is close to its value for diluted Gd^{3+} in LuInNi_4 , as reported previously.¹⁷ It is clear from these results that multiple band effects associated with the contribution of the Ni 3d bands are responsible for the increase of the b -rates, consistently with the results reported from the Gd^{3+} diluted LuInA_4 ($A = \text{Ni}, \text{Cu}$).¹⁷ As such, these effects may help to shed some light in the evolution of the magnetic properties in the GdInA_4 ($A = \text{Cu}, \text{Ni}$) series. In this sense, we must keep in mind that, in these compounds, (i) the RKKY magnetic interaction couples the Gd^{3+} magnetic moments determining their ground states and (ii) the analyses of X-ray patterns (see Fig. 1) show that the crystal structure of samples is not modified by the Ni-doping. Only small changes are observed in the lattice parameter giving no appreciable modification in the Gd-Gd distances. In this scenario, since the RKKY interaction is oscillatory and has a dependence with the distance of the magnetic moments, it is not unreasonable to suppose that the same ground state should be observed to, at least, the end members of $\text{GdIn}(\text{Ni}_x\text{Cu}_{1-x})_4$ compounds.

Interestingly, the analyses of the magnetization data shown in Figs. 2 and 3 are consistent with a change in the magnetic order from antiferromagnetic ($\Theta_{\text{CW}} < 0$) to ferromagnetic ($\Theta_{\text{CW}} > 0$). If one takes in mind that the high- T magnetic susceptibility obey to the Curie-Weiss law, $\chi(T) = \chi_0 + C/(T \pm \Theta_{\text{CW}})$, where χ_0 is a T -independent

susceptibility term, C is the Curie constant, and Θ_{CW} is the Curie-Weiss temperature. The enhancement of the susceptibility along the series of $\text{GdIn}(\text{Ni}_x\text{Cu}_{1-x})_4$ compounds strengthens our supposition once it should likely be related to the increase and change of sign of Θ_{CW} .

The change in the magnetic ground state can also be observed through isothermal magnetization curves. It notes that while the magnetization of Cu-based samples is linear up to the maximum magnetic field, the Ni-based samples reach a saturation for lower applied magnetic fields (~ 20 kOe), with a saturated magnetic moment of $6.9 \mu_B$.

The exchange parameter J evaluated from the T_N temperature using a mean field approximation ($T_N = nJ\mu_{\text{eff}}^2/3k_B$) yields $\approx 2 \times 10^{-6}$ eV. The magnetic potential energy ($E_M = -\mu_{\text{eff}} \cdot \mathbf{H}$) associated with the magnetic saturation is $\approx 7 \times 10^{-4}$ eV. If one supposes that the Ni-based samples are antiferromagnetically ordered, the above calculated energies should be the same. Also, Nakamura *et al.*²¹ have shown that GdInCu_4 reaches its saturation at magnetic fields around 300 kOe; hence, it is not acceptable to think that the saturation field decreases so drastically with a simple Cu-Ni substitution. If this is the case, the role of the Ni in the magnetic behavior of this family of compounds should be much more important. Besides confirming the transition temperatures observed in the T -dependence of susceptibility, the specific heat data for the Ni-rich samples are dominated by a sharp magnetic ordering peak at ≈ 4 K, which should be associated with the ferromagnetic transition. The calculated magnetic entropy [$S_m = R \ln(2J + 1) = R \ln(2S + 1) = R \ln 8$], is recovered by around 70% of the total entropy at T_N and no dependence in Ni-doping was observed. This is consistent with the existence of short-range correlations for our set of samples.

Finally, as we have commented above, the magnetic interaction between the localized magnetic moments in metallic samples can be well understood inside the RKKY approach, where the ce takes an important role. In this respect, the oscillatory character of RKKY interaction predicts a ferro or antiferromagnetic order depending on the distance between the localized magnetic moments.²⁶ In this sense, it seems unreasonable to think that the small changes in the lattice parameter observed along the series of $\text{GdIn}(\text{Ni}_x\text{Cu}_{1-x})_4$ compounds produce a dramatic change in the Gd-Gd, going from a negative to a positive exchange parameter.

In this scenario, the introduction of the Ni 3d bands, as revealed by the ESR data of Gd^{3+} diluted in a LuInNi_4 , can play an important role in the changes of the magnetic interactions. As we mentioned previously, ESR experiments of Gd^{3+} diluted in a LuInA_4 ($A = \text{Ni}, \text{Cu}$) host yield an exchange interaction, J_{fs} , between localized magnetic moment and ce is mainly positive for LuInNi_4 and negative for LuInCu_4 .¹⁷ One must remember that this result was associated with the different ce contributions: s and d electrons yielding positive values of g shift and J_{fs} for LuInNi_4 and s electrons yielding negative values of g shift and J_{fs} for LuInCu_4 . In the same way, a similar scenario seems to happen for $\text{GdIn}(\text{Ni}_x\text{Cu}_{1-x})_4$, where a gradual increase of Ni-doping seems to increase the d electron contribution, driving the system to change from

an antiferromagnetic ($J < 0$ for GdInCu_4) to a ferromagnetic ($J > 0$ for GdInNi_4) ground state. Despite the exchange interactions extracted from ESR experiments of Gd^{3+} diluted in a LuInA_4 ($A = \text{Ni, Cu}$)¹⁷ host and the Gd-Gd interaction in the concentrated compound are not the same, these ESR results suggest that the contribution of ce coming from different bands s , p , d , or even f should be considered in order to help in the understanding of the magnetic behavior of these compounds. Furthermore, the gradual change in the magnetic ground state from AFM to FM observed for the GdInA_4 ($A = \text{Cu, Ni}$) may explain the decrease of the magnetic frustration as a function of Ni concentration, since FM can be accommodated in a triangular lattice with no frustration (in contrast to AFM).

IV. CONCLUSIONS

In this work, single crystals of $\text{GdIn}(\text{Ni}_x\text{Cu}_{1-x})_4$ ($0.00 < x < 1.00$) have been synthesized via the flux method. The analyses of X-ray patterns indicate that all samples belong to a cubic symmetry similar to the AuBe_5 structure ($C15b$ -type structure). The lattice parameter slightly changes in the range of $7.08 \leq a \leq 7.23 \text{ \AA}$ along the series. The analysis of temperature dependent magnetization data indicate an evolution of the magnetic ground state from antiferromagnetic ($\Theta_{\text{CW}} < 0$) for Cu-rich samples to ferromagnetic ($\Theta_{\text{CW}} > 0$) for Ni-rich samples. Besides, the field-dependence of magnetization shows a linear behavior to Cu-rich samples and a saturation phenomenon to Ni-rich samples up to $H = 70 \text{ kOe}$. Since a simple analysis using the RKKY model based on Gd-Gd distances is not sufficient to explain the magnetic ground states of these compounds, we argue that such behavior can be ascribed to multiple band effects introduced by Ni-doping as revealed by the analysis of the Gd^{3+} ESR data.

ACKNOWLEDGMENTS

We thank the Brazilian agencies FAPESP-SP (Nos. 2012/04870-7, 2018/11364-7, and 2017/10581-1), FAPITEC (PRONEX) and CNPq (Nos. 455608/2014-8, 455970/2014-9, 442230/2014-1, and 304496/2017-0) for financial support. This study was financed in part by the Coordenação de Aperfeiçoamento de Pessoal de Nível Superior-Brasil (CAPES)-Finance Code 001.

REFERENCES

- ¹M. A. Ruderman and C. Kittel, *Phys. Rev.* **96**, 99 (1954).
²Y. Kei, *Phys. Rev.* **106**, 893 (1957).

- ³K. Tadao, *Prog. Theor. Phys.* **16**, 45 (1956).
⁴N. D. Mathur, F. M. Grosche, S. R. Julian, I. R. Walker, D. M. Freye, R. K. W. Haselwimmer, and G. G. Lonzarich, *Nature* **394**, 39 (1998).
⁵I. Feiner, I. Nowik, D. Vaknin, U. Potzel, J. Moser, G. M. Kalvius, G. Wortmann, G. Schmiester, G. Hilscher, E. Gratz, C. Schmitzer, N. Pillmayr, K. G. Prasad, H. de Waard, and H. Pinto, *Phys. Rev. B* **35**, 6956 (1987).
⁶K. Gofryk, J. C. Griveau, E. Colineau, J. P. Sanchez, J. Rebizant, and R. Caciuffo, *Phys. Rev. B* **79**, 134525 (2009).
⁷J. Spehling, R. H. Heffner, J. E. Sonier, N. Curro, C. H. Wang, B. Hitti, G. Morris, E. D. Bauer, J. L. Sarrao, F. J. Litterst, and H. H. Klaus, *Phys. Rev. Lett.* **103**, 237003 (2009).
⁸D. Kaczorowski, A. P. Pikul, D. Gnida, and V. H. Tran, *Phys. Rev. Lett.* **103**, 027003 (2009).
⁹E. C. T. O. Farrell, D. A. Tompsett, S. E. Sebastian, N. Harrison, C. Capan, L. Balicas, K. Kuga, A. Matsuo, K. Kindo, M. Tokunaga, S. Nakatsuji, G. Csányi, Z. Fisk, and M. L. Sutherland, *Phys. Rev. Lett.* **102**, 216402 (2009).
¹⁰V. R. Shaginyana, M. Ya. Amusiab, K. G. Popovc, and S. A. Artamonova, *JETP Lett.* **90**, 47 (2009).
¹¹P. Bonville, J. Hammann, J. A. Hodges, P. Imbert, and G. Jhanno, *J. Magn. Magn. Mater.* **151**, 115 (1995).
¹²P. D. Carfagna and W. E. Wallace, *J. Appl. Phys.* **39**, 5259 (1968).
¹³B. Politt, Ph.D. thesis, Universitat Koln, 1987.
¹⁴E. Bauer, E. Gratz, R. Hauser, Le. Tuan, A. Galatanu, A. Kottar, H. Michor, W. Perthold, G. Hilscher, T. Kagayama, G. Oomi, N. Ichimiya, and S. Endo, *Phys. Rev. B* **50**, 9300 (1994).
¹⁵J. L. Sarrao, R. Modler, R. Movshovich, A. H. Lacerda, D. Hristova, A. L. Cornelius, M. F. Hundley, J. D. Thompson, C. L. Benton, C. D. Immer, M. E. Torelli, G. B. Martins, Z. Fisk, and S. B. Oseroff, *Phys. Rev. B* **57**, 7785 (1998).
¹⁶C. Kittel, *Quantum Theory of Solids* (Wiley, New York, 1987).
¹⁷P. G. Pagliuso, C. Rettori, J. L. Sarrao, A. Cornelius, M. F. Hundley, Z. Fisk, and S. B. Oseroff, *Phys. Rev. B* **60**, 13515 (1999).
¹⁸K. Kojima, Y. Nakai, T. Suzuki, H. Asano, F. Izumi, T. Fujita, and T. Hihara, *J. Phys. Soc. Jpn.* **59**, 792 (1990).
¹⁹H. Nakamura, N. Kim, M. Shiga, R. Kmieć, K. Tomala, E. Ressouche, J. P. Sanchez, and B. Malaman, *J. Phys. Condens. Matter* **11**, 1095 (1999).
²⁰V. Fritsch, J. D. Thompson, and J. L. Sarrao, *Phys. Rev. B* **71**, 132401 (2005).
²¹H. Nakamura, K. Ito, H. Wada, and M. Shiga, *Physica B* **186-188**, 633 (1993).
²²A. Severing, E. Gratz, B. D. Rainford, and K. Yoshimura, *Physica B* **163**, 409 (1990).
²³A. Abragam and B. Bleaney, *EPR of Transition Ions* (Clarendon Press, Oxford, 1970).
²⁴M. Cabrera-Baez, V. C. Denis, L. Mendona-Ferreira, M. Carlone, P. A. Venegas, M. A. Avila, and C. Rettori, *Phys. Rev. B* **97**, 224425 (2018).
²⁵P. G. Pagliuso, C. Rettori, S. B. Oseroff, J. Sarrao, Z. Fisk, A. Cornelius, and M. F. Hundley, *Solid State Commun.* **104**, 223 (1997).
²⁶J. Jensen and A. R. Mackintosh, *Rare Earth Magnetism* (Clarendon, Oxford, 1991).